ARMY RESEARCH LABORATORY

Morphology and Morphological Changes Within Nafion Membranes Induced by Mechanical Orientation

by S. F. Trevino and Sandra K. Young

ARL-TR-2700 November 2002

NOTICES

Disclaimers

The findings in this report are not to be construed as an official Department of the Army position unless so designated by other authorized documents.

Citation of manufacturer's or trade names does not constitute an official endorsement or approval of the use thereof.

Destroy this report when it is no longer needed. Do not return it to the originator.

Army Research Laboratory
Aberdeen Proving Ground, MD 21005-5069

ARL-TR-2700 **November 2002**

Morphology and Morphological Changes Within Nafion Membranes Induced by Mechanical Orientation

S. F. Trevino and Sandra K. Young
Weapons and Materials Research Directorate, ARL

Abstract

The structure of Nafion, a perfluorosulfonated ionomer, has been the subject of many studies. Morphology evaluations have used the methods of small-angle x-ray scattering (SAXS), wide-angle x-ray scattering (WAXS), and small-angle neutron scattering (SANS). Three principal features in the small-angle scattering pattern have been observed on the H^+-form Nafion. A peak at approximately Q ~0.2 $Å^{-1}$ is attributed to the clustering of the acid groups (ionomer peak), that at Q ~0.03 $Å^{-1}$ to crystalline regions, and an upturn in intensity at the smallest Q to large-scale heterogeneities. Some of the previous works have included samples that have experienced moderate strains by mechanical elongation. In those works, the effect on the ionomer peak has been studied. The WAXS studies led to a model of the packing of the polymer molecules into ionic aggregates, while the SAXS and SANS studies resulted in models of the packing of the ionic clusters. In the present work, SANS measurements on elongated samples of Nafion have been used to obtain data that suggests a model of the structure of the material. The samples studied were elongated at two temperatures, 25° and 155 °C. Although many of the scattering features of these two samples are similar, the samples stretched at 155 °C contain new information concerning the nature of the crystalline region.

Acknowledgments

The authors would like to thank the following individuals for their assistance with this effort:

- Paul Moy of the U.S. Army Research Laboratory, Weapons and Materials Research Directorate, Polymers Research Branch, for help with the mechanical stretching of samples,
- Dr. Thomas Gnaeupel-Herold for help in the collection and interpretation of the pole figure data,
- Dr. Edward Prince for general crystallographic guidance, and
- Frederick L. Beyer for useful discussions.

In addition, the authors would like to acknowledge the use of the facilities at the National Institutes of Standards and Technology (NIST) Center for Neutron Research where all of the small-angle neutron scattering (SANS) and diffraction experiments were performed. Also, the American Association for Engineering Education Post-Doctoral Research Associate Program and the U.S. Army Natick Soldier Center are acknowledged for financial support to author Sandra K. Young.

INTENTIONALLY LEFT BLANK.

Contents

Acknowledgments iii

List of Figures vii

List of Tables ix

1. Introduction 1

2. Experimental 2

2.1 Materials 2

2.2 Initialization 2

2.3 Mechanical Tensile Testing 2

2.4 SANS 3

2.5 Prompt Gamma Neutron Activation Analysis 3

3. Results 3

3.1 The Ionic Region 4

3.2 The Crystalline and Intraparticle Features 10

4. Discussion 12

5. Conclusions 15

6. References 17

Report Documentation Page 21

INTENTIONALLY LEFT BLANK.

List of Figures

Figure 1. The chemical structure of Nafion. 1

Figure 2. The scattering cross section from the three undeformed Nafion samples. The two labeled 155° and 25 °C were recovered from the undistorted parts of the samples held in the jaws of the stretching machine. 4

Figure 3. The SAS pattern obtained from (a) the sample stretched to $dL/L_o = 5.1$ at 25 °C and (b) the sample stretched to $dL/L_o = 15.9$ at 155 °C. The circle is drawn for a $Q = 0.12$ Å^{-1}. Here the short camera configuration is used in order to obtain scattering at the largest values of Q. The stretch direction is approximately vertical. 5

Figure 4. The horizontal sector average of the data of Figure 3 (a) and (b). The notation identifying the two patterns refer to the conditions of deformation as described in the text. The solid lines correspond to the background and peaks describing the data. 6

Figure 5. A plot of Q_o, the peak positions, vs. dL/L_o, the strain, for the various deformed samples. The temperature labels refer to the temperature at which the material was deformed. The straight lines serve as guides to the eye. 7

Figure 6. The standard deviations plotted against the strain dL/L for several samples. The lines serve as guides to the eye. 8

Figure 7. The annular averages of the data of Figure 3 (a) and (b). The labels of the data are as discussed in section 2.3. The horizontal corresponds to $\phi = 0$. The slight shift of the peak from $\phi = 0$ reflects a misorientation of the sample upon mounting. The value of Q at which the average is centered corresponds to the peak value Q_o of Table 1. 9

Figure 8. Plots of I, the integrated intensity, and σ (degrees), the standard deviation, resulting from fits of annular averages as functions of the strain $\Delta L/L$. The data corresponding to the samples strained at the two temperatures are so labeled. The lines are present to serve as guides to the eye. 10

Figure 9. The medium Q camera configuration of the SANS obtained from the sample stretched to $\Delta L/L_o = 15.9$ at 155 °C. 11

Figure 10. The sector average along the horizontal of the samples stretched at the two temperatures and strains indicated. The solid lines are fits to the data with a Guinier function resulting in the values of Rg, the radius of gyration, as listed in the figure. 12

Figure 11. The Q values of the major (horizontal) and minor (vertical) axes which describe the elliptical diffraction pattern of the samples stretched at 155 °C (see Figure 9) as a function of dL/L_o. The figure at right presents the corresponding lattice constant d. The lines are a guide to the eye. 13

Figure 12. A schematic of the proposed model of the structure of stretched Nafion 14

List of Tables

Table 1. The results of Gaussian fits to the ionomer peak of the various deformed samples.....7

Table 2. The result of fits to the annular data obtained for the various samples as discussed in section 2.3. 9

INTENTIONALLY LEFT BLANK

1. Introduction

Nafion is a commercial synthetic perfluorosulfonated ionomer produced by the E. I. du Pont de Nemours Company. Its stoichiometry is shown in Figure 1. The sulfonic acid groups are strongly hydrophilic and attract each other through Coulombic interactions. Thus, even when dry, aggregates can be formed by the association of these groups. The existence of the aggregates has been inferred from the presence of a peak in the small-angle scattering (SAS) of both x-rays and neutrons. This ionic peak is located at Q ~0.2 $Å^{-1}$ ($Q = 4\pi \sin(\theta)/\lambda$, where 2θ is the scattering angle, and λ is the wavelength of the radiation). The position of this peak in Q is a function of solvent content (water, various alcohols, and other liquids), and thermal and mechanical treatment. The fact that its position is a strong function of solvent content justifies making its assignment to aggregates formed by the acid groups and adsorbed solvents. It has been the goal of many studies [1–15] to describe the geometry of these aggregates. Several of these studies have been performed on stretched samples [5, 9, 12–15]; however, a definitive model is difficult to defend from the properties of only one peak. This situation is, of course, familiar to the polymer community. It is therefore desirable to obtain data of significantly different qualitative properties that might lend credence to a particular model. In addition to the ionic peak, there exist two other features in the SAS. A peak at Q ~0.03 $Å^{-1}$ has been attributed to crystalline regions in the material and a strong upturn in the scattering intensity as Q tends toward zero, to large-scale fluctuations.

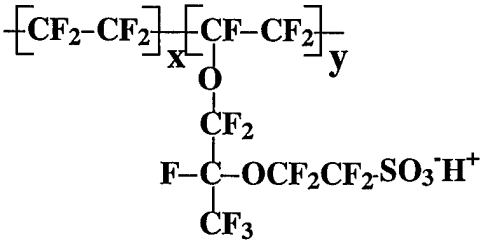

Figure 1. The chemical structure of Nafion.

In our work, we wish to add substantial experimental data to this problem by obtaining neutron diffraction pole figures and high-resolution small-angle neutron scattering (SANS) data from samples of Nafion, which have been extensively deformed by mechanical stretching.

2. Experimental

2.1 Materials

Perfluorosulfonate ionomer membranes (PFSI) in the SO_3H form (Nafion 117) were obtained from C. G. Processing, Inc.* The membranes had an equivalent weight of 1100 g/equiv (7 mil [175 μm] thick) and correspond to ~13 CF_2 groups between the side chains. Concentrated hydrochloric acid (HCl), and concentrated nitric acid (HNO_3) were obtained from VWR Scientific† and used as received. All water utilized was distilled and deionized (DI/DS).

2.2 Initialization

Some membranes in this work are referred to as initialized, pretreating the membranes by the procedure reported by Davis et al. [16]. As-received membranes were exchanged to the acid form by refluxing in 50% HCl:50% HNO_3 solution (v:v), leaching out excess acid in deionized water reflux (three times), and finally vacuum drying at 125 °C. All membranes were exchanged to this standard initialized state prior to counterion exchange, and prompt gamma analysis was used in order to assure maximum sample reproducibility.

2.3 Mechanical Tensile Testing

Tensile tests were conducted on a computer-controlled Instron‡ screw drive electromechanical load frame. Installed on the load frame is a high-temperature Instron oven for the elevated temperature tests. A set of spring-loaded clamping grips designed for high-elongation materials, such as elastomers, were used in the test. These grips also have rubber-coated rollers, rather than a serrated face, to prevent premature and unwanted rupture of the specimens at the grip interface. Instron proprietary software, series IX, was used to control and to provide data acquisition for each test.

Deformation of the membranes was produced with the Instron machine at two temperatures: 25° and 155 °C. The stretching rate was 0.02 mm/s. At each temperature, the material was stretched until it broke in order to determine the maximum strain which could be sustained. The result is that at 25 °C maximum strain is $\Delta L/L_o$ ~5, and at 150 °C maximum strain is $\Delta L/L_o$ ~15.9. Subsequently, samples were produced at several values of $\Delta L/L_o$ up to nearly the maximum at each temperature. In each of these, $\Delta T/T_o$ (T being the thickness) decreased by

* C. G. Processing, Inc., P.O. Box 133, Rockland, DE 19732.

† VWR Scientific Products, 405 Heron Drive, P.O. Box 626, Bridgeport, NJ 08014.

‡ Model 4505.

an amount ~7% of that of $\Delta L/L_o$. These were then used in the diffraction and SANS studies.

2.4 SANS

The SANS measurements were accomplished using the 30-m instrument located at NG7 of the Cold Neutron Research Facility (CNRF) of the National Institute of Standards and Technology (NIST) [17]. A neutron wavelength of 5 Å and several camera configurations were used in order to obtain data over a large range of Q (0.006–0.7 $Å^{-1}$). Several aligned layers of the samples were used to obtain samples of approximately 1-mm thickness. All spectra were corrected for both empty and blocked sample backgrounds. The absolute macroscopic scattering cross section was obtained by comparison with a measurement of the incident beam intensity.

2.5 Prompt Gamma Neutron Activation Analysis

The prompt gamma spectrometer [18] on NG7 of the CNRF was employed to determine the water content of the samples. For now, it is sufficient to state that the atomic ratio of hydrogen to sulfur can be determined to an accuracy of 1–2%.

3. Results

Several of the deformed samples were investigated with the prompt gamma instrument and all were found to contain, on average, three water molecules per sulfonic acid. This is consistent with other studies of the amount of water adsorbed by the Nafion exposed to moderate relative humidity [19].

All of the SANS spectra were obtained with the incident neutron beam perpendicular to the membrane surface and the stretch direction vertical. SANS spectra of three samples of the undeformed polymer also were obtained. These consisted of the as-received material and that of the initialized material recovered from the jaws of the stretching machine for the two temperatures used in the deformation process, 25° and 155 °C, respectively. The scattering pattern for the three samples was essentially cylindrically symmetric about the incident beam direction. Circular average of this data is presented in Figure 2.

It is clear that, although the general features in the spectra of the three samples are present, the specifics are sensitive to the chemical and thermal treatment. Both the ionic and crystalline peaks of the initialized samples move to smaller values of Q (larger spacing) with respect to the as-received sample. It is possible that steric effects (which can be overcome with thermal energy and chemical treatment) prevent the relaxation of the material into its minimum energy structure at ambient temperature.

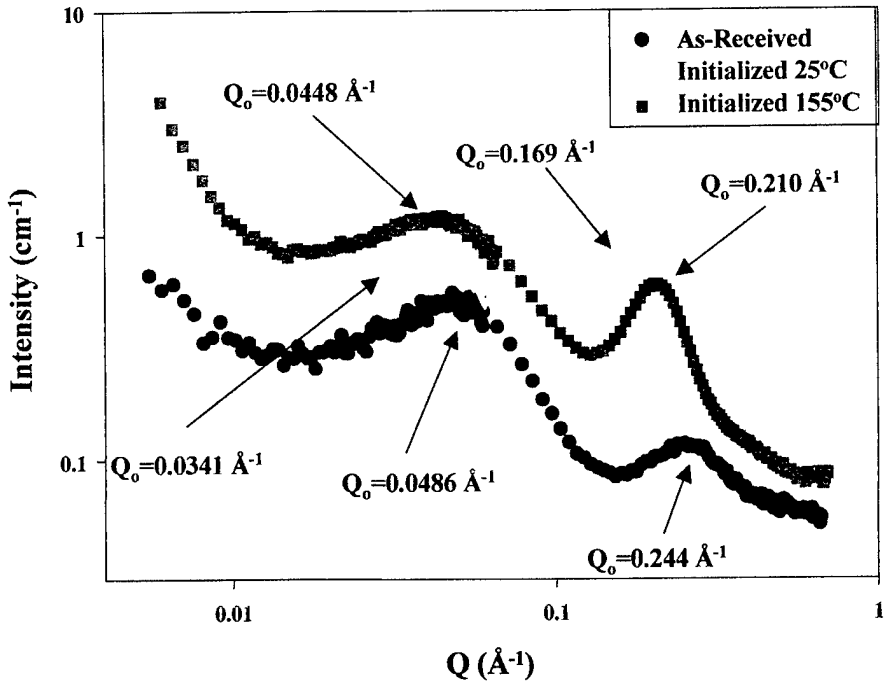

Figure 2. The scattering cross section from the three undeformed Nafion samples. The two labeled 155° and 25 °C were recovered from the undistorted parts of the samples held in the jaws of the stretching machine.

Figure 3 presents false color representations of the neutron intensity data collected by the two-dimensional (2-D) detector of the 30-m SANS instrument. Figure 3(a) is that stretched to $dL/L_o = 5.1$ at a temperature of 25 °C, and Figure 3(b) is that for the sample stretched to $dL/L_o = 15.9$ at a temperature of 155 °C. The sample temperature at the time of the SANS measurement is ambient. In both cases, the stretch direction is approximately vertical.

Two regions of Q will be discussed separately. The diffraction intensity for values of $Q \geq 0.12$ Å^{-1} describes the properties of the ionic structure, whereas that for $Q \leq 0.12$ Å^{-1} describes the crystalline and intraparticle features. The blue circle in Figure 3(b) delineates these two regions.

3.1 The Ionic Region

It is clear from Figure 3 (a) and (b) that the process of stretching has affected the spatial orientation of the structure giving rise to the feature at Q ~0.2 Å^{-1}. This effect has been observed previously [5, 9, 12-15]. Appropriate averages of the 2-D data will be used to describe the effect of stretching the membrane. A sector average of the data with an angular width of 5° allows the determination of peak position, intensity and Q width. An annular average, with the annulus centered

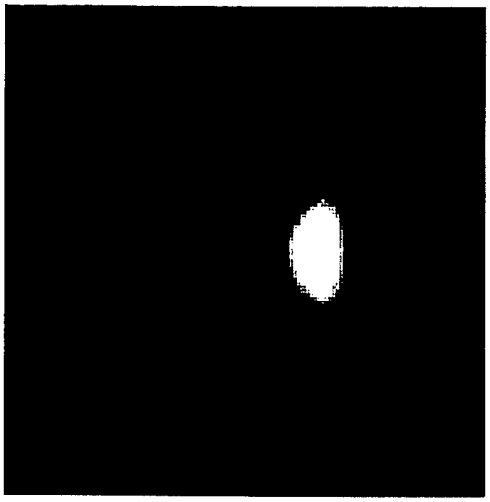

(a)

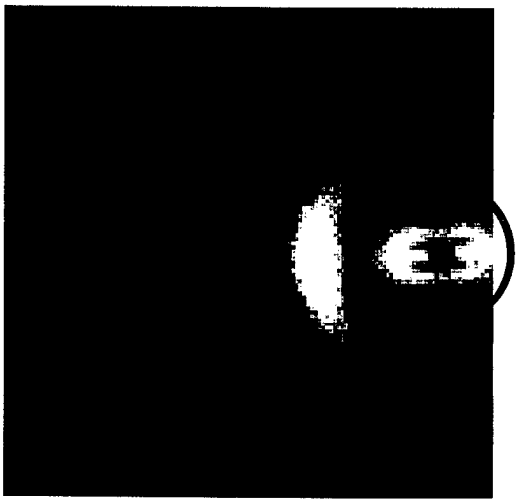

(b)

Figure 3. The SAS pattern obtained from (a) the sample stretched to $dL/L_o = 5.1$ at 25 °C and (b) the sample stretched to $dL/L_o = 15.9$ at 155 °C. The circle is drawn for a $Q = 0.12$ Å^{-1}. Here the short camera configuration is used in order to obtain scattering at the largest values of Q. The stretch direction is approximately vertical.

at the Q value corresponding to the peak position and of width equal to, say, the half maximum width of the peak, will reveal the degree of spatial orientation achieved by stretching.

Figure 4 presents a sector average in a horizontal direction, of each of the two data sets of Figure 3 (a) and (b). The data has been fit with a Gaussian function for each of the peaks and a general function describing the severely sloping background. Both the background and the several peak fits are shown in the

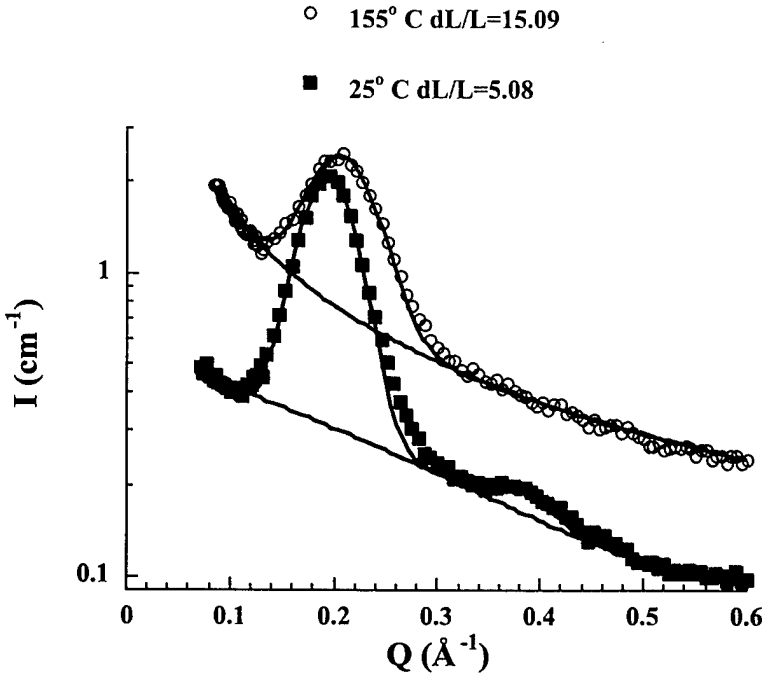

Figure 4. The horizontal sector average of the data of Figure 3 (a) and (b). The notation identifying the two patterns refer to the conditions of deformation as described in the text. The solid lines correspond to the background and peaks describing the data.

figure. The data for the cold stretch sample shows two peaks. These occur at values of Q of 0.194 and 0.388 Å^{-1}, respectively, differing by exactly a factor of 2. It is tempting to assign the second peak as the order of the first. However, data on undeformed samples as a function of volume fraction of various solvents also produces the two peaks but not in the Q ratio of 2 to 1 [20]. Both peaks do move with volume fraction so that they may represent different features of the mechanism of solvation. Although the sector-averaged scattering curve of the sample stretched at 155 °C does not show the high Q peak, a circular average of the data does exhibit its presence. In any case, the parameters describing the larger of these two peaks, i.e., the one associated as the ionic peak, have been determined for all of the deformed samples. These values are presented in Table 1.

It is interesting to plot some of this data. Thus, Figure 5 is the plot of Q_o as a function of dL/L_o for the samples stretched at the two temperatures. Inspection of this figure reveals that the material stretched at the elevated temperature attains the equilibrium value of the peak position at the smallest deformation obtained here, whereas that stretched at ambient temperatures does not. The deformation of the latter sample does change the peak position in a manner that tends toward that of the former. Both of these effects suggest that the equilibrium value of Q_o is ~0.21 Å^{-1}.

Table 1. The results of Gaussian fits to the ionomer peak of the various deformed samples.

dL/L	T (°C)	I_o	Q_o (Å^{-1})	σ(Q) (Å^{-1})
0.00	22.0	–	0.173	0.0343
1.04	22.0	0.0585	0.185	0.0349
2.05	22.0	0.0747	0.192	0.0324
2.98	22.0	0.0771	0.191	0.0325
4.06	22.0	0.0830	0.194	0.0326
5.09	22.0	0.096	0.195	0.0319
0.00	155.0	–	0.208	0.0338
2.35	150.0	0.0403	0.212	0.0343
5.49	152.0	0.0413	0.211	0.0340
8.71	152.0	0.0427	0.211	0.0339
11.4	154.0	0.0423	0.210	0.0340
15.9	155.0	0.0498	0.208	0.0339

Notes: dL/L is the strain, T the temperature at which the samples were strained, I_o the integrated intensity, Q_o the peak position, and σ(Q) the standard deviation from the fit.

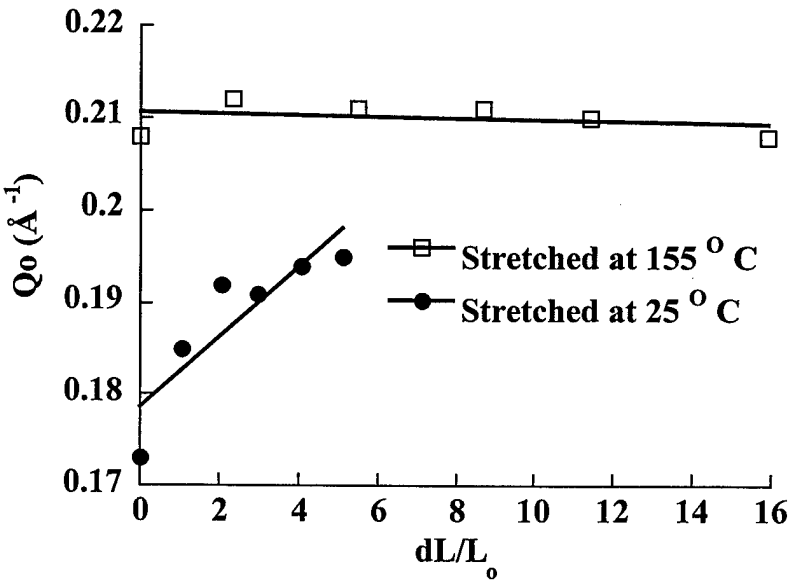

Figure 5. A plot of Q_o, the peak positions, vs. dL/L_o, the strain, for the various deformed samples. The temperature labels refer to the temperature at which the material was deformed. The straight lines serve as guides to the eye.

A second parameter, which yields information on the effect of stretching, is σ, the standard deviation resulting from the Gaussian fit of the peak. This parameter is plotted in Figure 6 as a function of dL/L_o, the strain produced on the several samples. Although the absolute change is not large, the different trends, produced in the samples stretched at the two temperatures, is significant. This behavior is consistent with the competition between the entropically and thermodynamically favored arrangements of polymer systems.

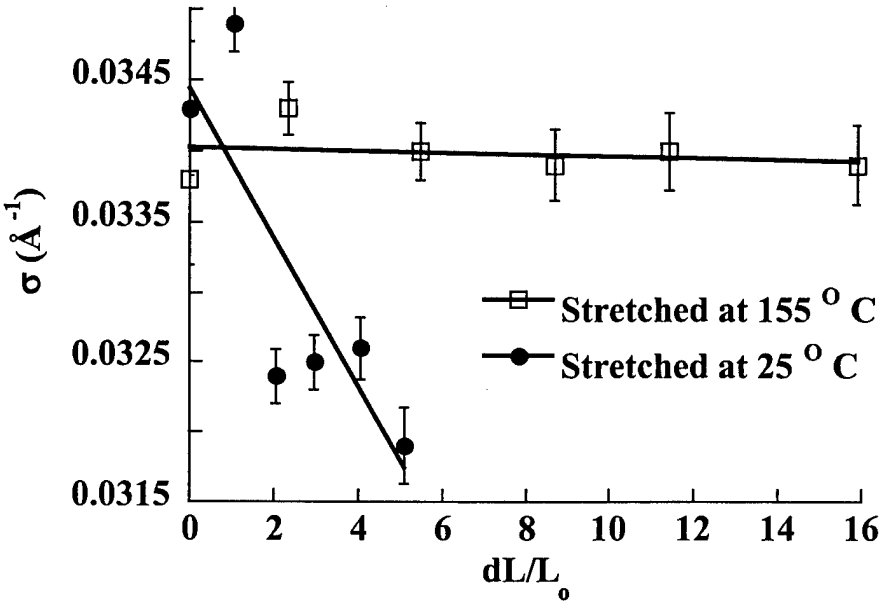

Figure 6. The standard deviations plotted against the strain dL/L for several samples. The lines serve as guides to the eye.

Annular averages are obtained for the data of Figure 3 (a) and (b) and are presented in Figure 7. It is clear from the figure that all the features correspond to a spatial orientation due to the deformation. The solid lines are fits with a Gaussian function. The parameters, which describe the Gaussian corresponding to these functions, are given in Table 2 along with those obtained for the various other deformed samples. In this table, only the data for the intense ionic peak is given. I, the integrated intensity, and σ, the standard deviation (in degrees) obtained from the Gaussian fit data, are plotted in Figure 8 as functions of $\Delta L/L_o$, the strain. Here again, the effect of strain on the sample is dramatically different when applied at different temperatures. Both parameters indicate that the cold stretched sample produces a greater degree of orientation of the structure represented by this feature.

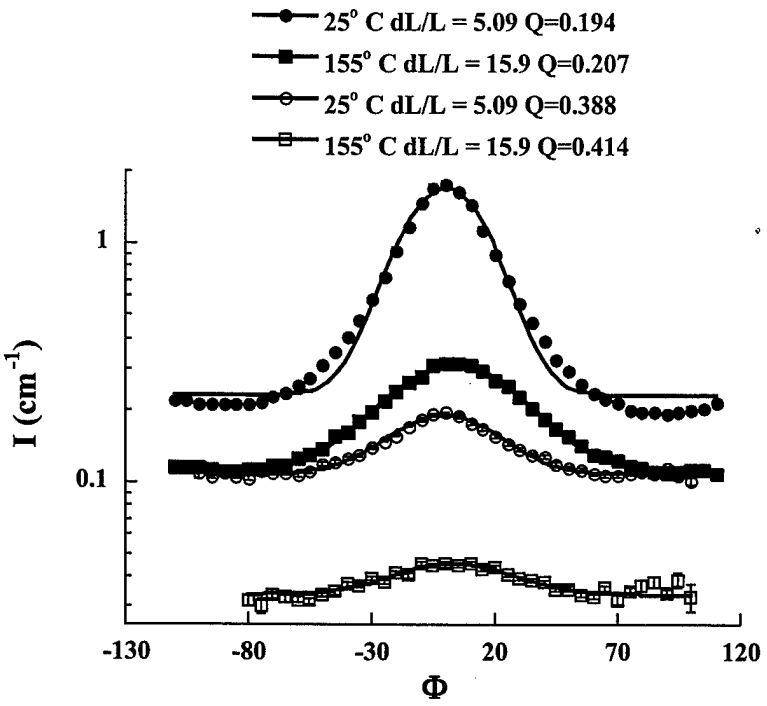

Figure 7. The annular averages of the data of Figure 3 (a) and (b). The labels of the data are as discussed in section 2.3. The horizontal corresponds to $\phi = 0$. The slight shift of the peak from $\phi = 0$ reflects a misorientation of the sample upon mounting. The value of Q at which the average is centered corresponds to the peak value Q_o of Table 1.

Table 2. The result of fits to the annular data obtained for the various samples as discussed in section 2.3.

dL/L	T (°C)	I	error	σ	error
1.04	25	47.3	0.40	28.1	0.20
2.05	25	52.7	0.69	20.2	0.25
2.98	25	54.9	0.69	20.0	0.24
4.06	25	56.6	0.89	18.5	0.28
5.09	25	62.5	1.2	17.0	0.31
2.35	155	26.3	0.31	31.3	0.29
5.49	155	23.0	0.18	29.5	0.19
8.71	155	12.5	0.10	27.2	0.19
11.4	155	12.2	0.14	25.5	0.26
15.9	155	12.9	0.17	25.8	0.29

Notes: dL/L and T are as in Table 1, and I and σ are the integrated intensity and standard deviation, respectively, with their corresponding errors.

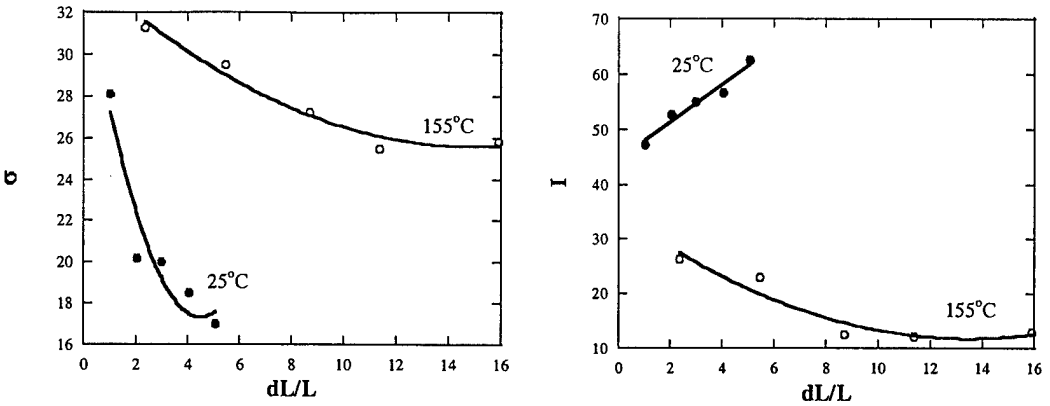

Figure 8. Plots of I, the integrated intensity, and σ (degrees), the standard deviation, resulting from fits of annular averages as functions of the strain ΔL/L. The data corresponding to the samples strained at the two temperatures are so labeled. The lines are present to serve as guides to the eye.

If we interpret the value of Q_o as reflecting the distance between the structures causing the diffraction, then $d = 2\pi/Q_o$ is ~30 Å. The width of the diffraction line reflects a correlation length over which this structure persists and using the Scherrer [21] equation this minimum length is $[\pi/\sigma(Q)\sqrt{(2\ln 2)}]$ ~80 Å corresponding to approximately four such structures. We may postulate that these structures are composed of those proposed by Starkweather [22]. They are aligned with the chain axis parallel to the stretch direction and assembled approximately four wide in a direction perpendicular to the stretch direction. The model discussed in section 4 will make these statements clear.

3.2 The Crystalline and Intraparticle Features

Examination of the low Q region of Figure 3 (a) and (b) reveals a dramatic difference in the spectrum of the two samples. Both exhibit a horizontal streak perpendicular to the stretch direction which passes through Q = 0. This type of scattering is characteristic of intraparticle interference by an elongated structure [23]. The horizontal direction of the streak corresponds to a vertical orientation of the elongated structure with its long axis parallel to the stretch direction. In the scattering pattern from the hot stretched sample, there appears an additional feature resembling an ellipse surrounding the main beam direction. For clarity, Figure 9 presents regions of Q, for this sample, obtained with a camera configuration adjusted to magnify these features. To our knowledge, these features have not been observed previously.

Let us first examine the horizontal streak passing through Q = 0. A sector average of the data from both samples along the horizontal direction produces the data of Figure 10. Here the labeling is as before. The solid lines are Guinier fits to the data with the resulting values of Rg as indicated in the figures. The

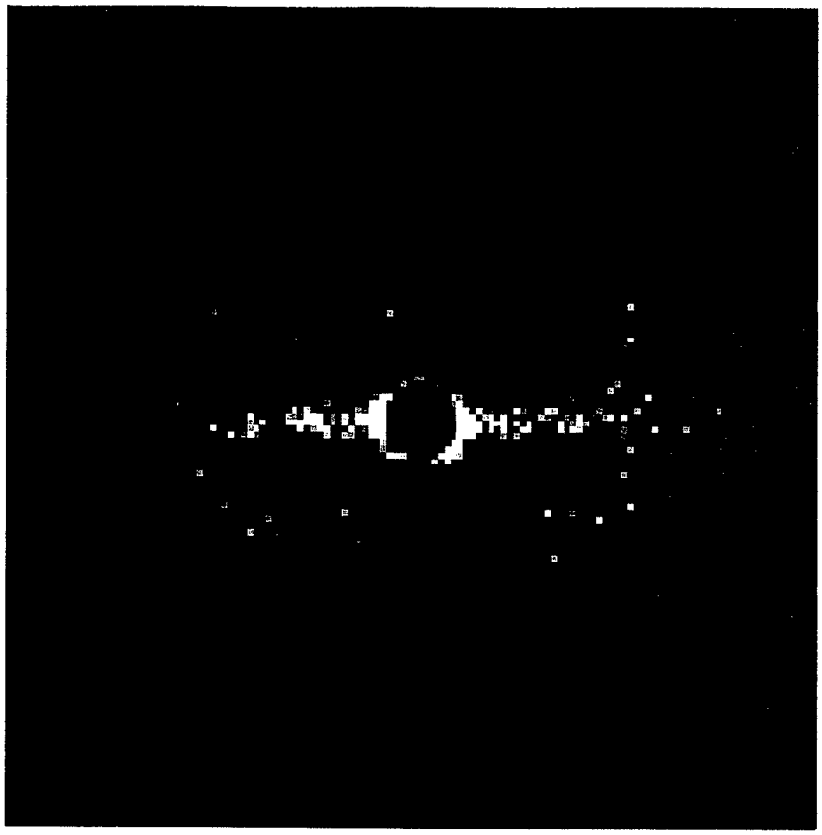

Figure 9. The medium Q camera configuration of the SANS obtained from the sample stretched to $\Delta L/L_o = 15.9$ at 155 °C.

data parallel to the stretch direction are not adequate to obtain a value of Rg for the long axis. It must however be rather large.

The elliptical-like feature clearly originates from a diffraction effect. This feature is not present in the pattern produced by the sample strained at low temperature (see Figure 2). The Q dependence on ϕ is well described by an ellipse. The major (horizontal) and minor (vertical) axes have been determined from the spectra for the several values of dL/L_o. These and the corresponding lattice spacings are presented in Figure 11. It is more difficult to obtain the dependence on ϕ of the intensity of the scattering. There is, at small values of ϕ, substantial interference from the central streak. If we assume, by inspection of Figure 9, that the maximum occurs at $\phi = 0$ but use only the data for $\phi > 40°$, we find a width of ~60° for the angular distribution. In all the undeformed samples, there exists a ring of scattering in the vicinity of this value of Q. Clearly, this crystalline ordering exists in the undeformed samples, although randomly oriented. In that stretched at 155 °C the array persists upon stretching, although distorted. The cold stretching destroys this order.

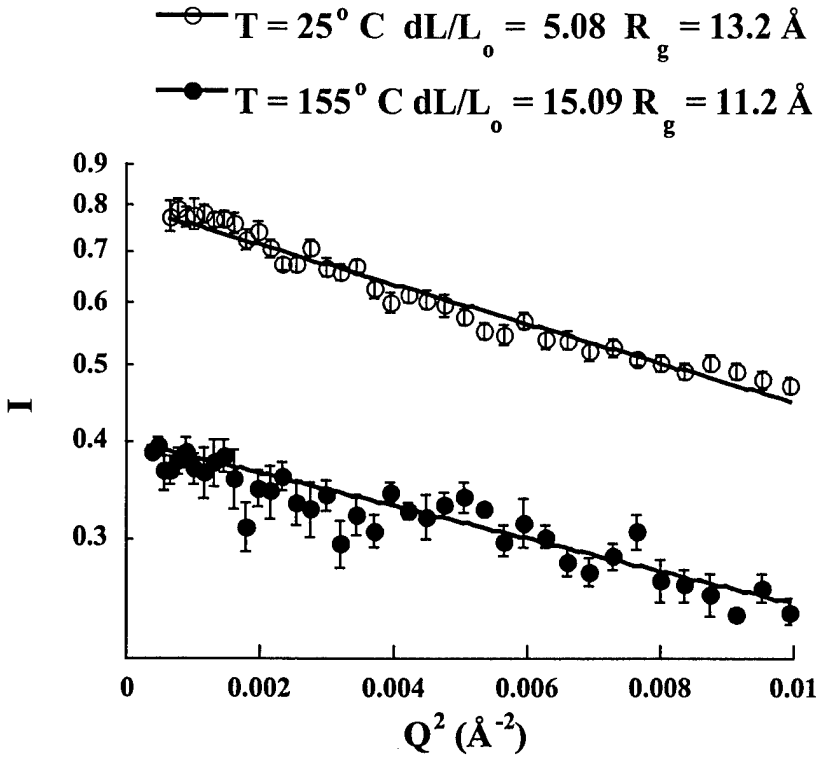

Figure 10. The sector average along the horizontal of the samples stretched at the two temperatures and strains indicated. The solid lines are fits to the data with a Guinier function resulting in the values of Rg, the radius of gyration, as listed in the figure.

4. Discussion

The central streak in the scattering pattern of samples deformed at both temperatures corresponds to a value of Rg ~12 Å. This translates to a diameter of approximately 30-35 Å for the object depending on the shape. The precise shape of the structure cannot be deduced simply from this scattering pattern [23]. However, it is elongated along the stretch direction, and the dimension previously given corresponds to that in the horizontal direction. The length of the object along the stretch direction must be substantially larger than its width.

The ionic peak is a diffraction peak arising from a lattice of spacing ~30 Å (from the average value of Q_o) with a coherence length of 80 Å (from the width of the peak). This lattice is partially ordered and oriented perpendicular to the stretch direction. We postulate that the mechanism of ordering is that of rotating the structure upon stretching. The disorder of the chain direction with respect to the

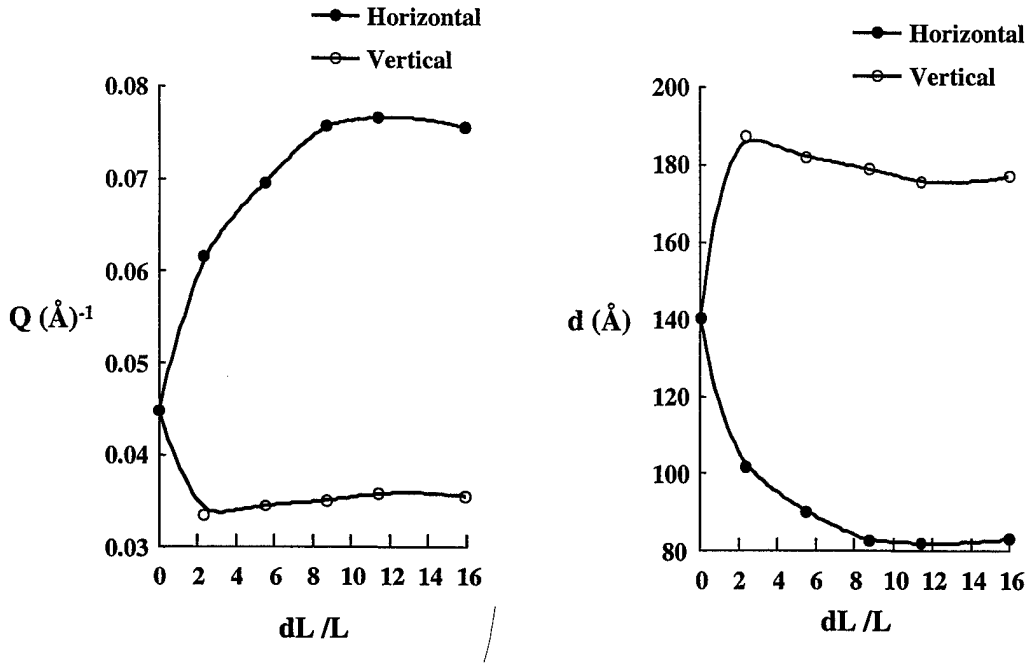

Figure 11. The Q values of the major (horizontal) and minor (vertical) axes which describe the elliptical diffraction pattern of the samples stretched at 155 °C (see Figure 9) as a function of dL/L_o. The figure at right presents the corresponding lattice constant d. The lines are a guide to the eye.

stretch direction is ~25°. This is very similar to the disorder presented by the array of parallelepipeds, which results in the ionic peak. The ionic peak results from the 30-Å spacing. The fact that the disorder of the chains and of the parallelepipeds is very similar may not be fortuitous.

The crystalline structure, as reflected by the smallest Q feature, is of monolithic lattice constant in the undeformed samples ranging from 140 to 180 Å depending on the treatment (see Figure 2). This structure is severely distorted by the deformation when applied at 155 °C and eliminated when applied at 25 °C. The mechanism responsible for this latter effect may be also responsible for the asymmetry in the intensity of the structure in the hot stretched sample. In the cold stretched sample, complete melting of this structure is achieved, whereas in the hot stretched sample, only in the maximum deformed direction is partial melting achieved.

Figure 12 is a schematic which reflects the previously mentioned geometric constraints for the hot stretched sample. The rectangular parallelepiped represents the arrangement of the backbone chains. These are shown as the zigzag figures in one of the parallelepipeds.* These parallelepipeds assemble in the larger structures whose dimensions are reflected in the ionomer peak. The

* This is the arrangement of the polymer chains proposed by Starkweather [22].

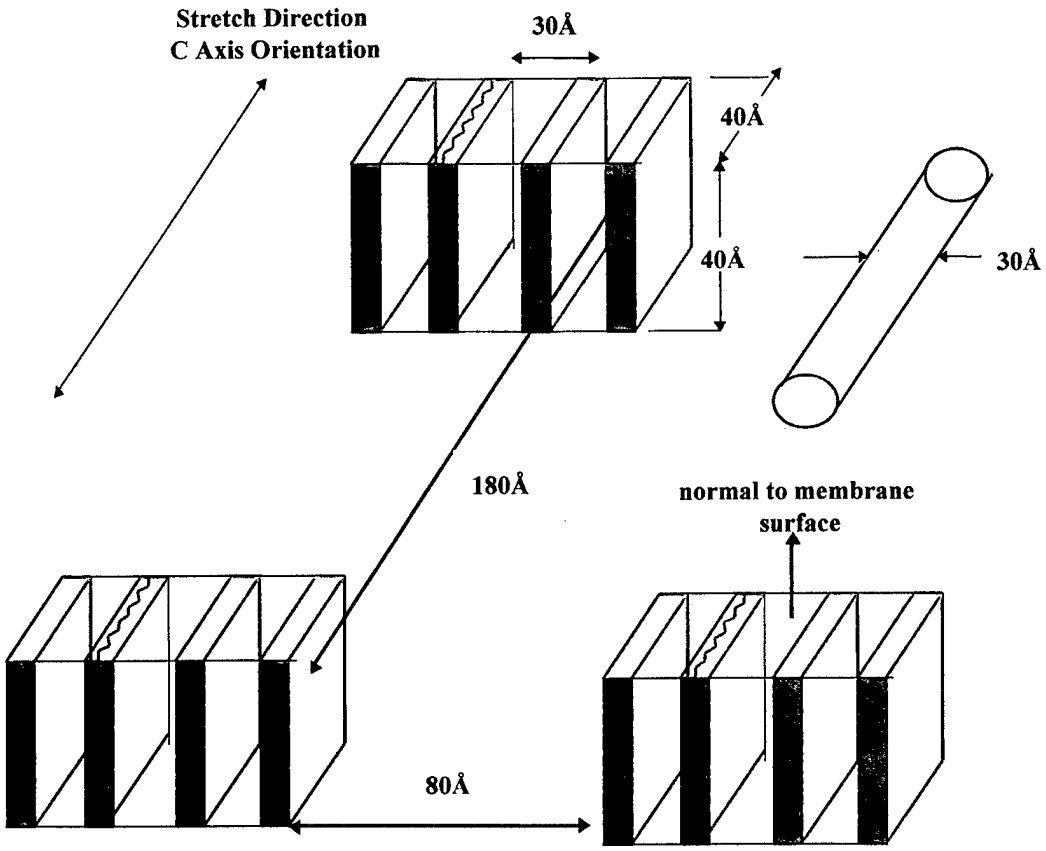

Figure 12. A schematic of the proposed model of the structure of stretched Nafion.

largest regular assembly is represented by the relative placement of the three smaller structures. The orientation of the entire array with respect to the stretch direction and the membrane surface is suggested by the asymmetric intensity distribution of the various reflections and is only the most probable. The distance between these largest structures is, of course, a function of the angle with respect to the stretch direction (Figure 9).

The cylinder is meant to represent the structure that gives rise to the horizontal streak. It is difficult to estimate the number density and length of this structure from the data. This orientation of the structure is present only in the deformed samples and is probably the deformation of the uniformly distributed "large scale fluctuations" present in the undeformed samples. We conclude that the amorphous regions become ordered upon deformation. The fact that a substantial scattering occurs reflects the presence of the sulfonic acid side groups that provide the necessary contrast.

5. Conclusions

We believe that the new data presented here leads to a reasonable model of the structure of Nafion. This structure is also consistent with the changes observed in the ionic peak as a function of solvent content. This structure is closer to that proposed by Litt [24] than others. The model suggests that in the deformed samples, properties such as permeability and electrical conductivity might exhibit substantial asymmetry with respect to both the stretch direction and the membrane surface.

INTENTIONALLY LEFT BLANK.

6. References

1. Roche, E. J., R. S. Stein, T. P. Russell, and W. J. MacKnight. "Small-Angle X-ray Scattering Study of Ionomer Deformation." *Journal of Polymer Science Polymer Physics Edition*, vol. 18, pp. 1497–1512, 1980.

2. Roche, E. J., M. Pineri, R. Duplessix, and A. M. Levelut. "Small-Angle Scattering Studies of Nafion Membranes." *Journal of Polymer Science Polymer Physics Edition*, vol. 19, pp. 1–11, 1981.

3. Gierke, T. D., G. E. Munn, and F. C. Wilson. "The Morphology in Nafion Perfluorinated Membrane Products, as Determined by Wide- and Small-Angle X-ray Studies." *Journal of Polymer Science Polymer Physics Edition*, vol. 19, pp. 1687–1704, 1981.

4. Fujimura, M., T. Hashimoto, and H. Kawai. "Small-Angle X-ray Scattering Study of Perfluorinated Ionomer Membranes. 1. Origin of Two Scattering Maxima." *Macromolecules*, vol. 14, pp. 1309–1315, 1981.

5. Fujimura, M., T. Hashimoto, and H. Kawai. "Small-Angle X-ray Scattering Study of Perfluorinated Ionomer Membranes. 2. Models for Ionic Scattering Maximum." *Macromolecules*, vol. 15, pp. 136–144, 1982.

6. Rebrov, A. V., A. N. Ozerin, A. N. Yakunin, N. A. Dreiman, S. V. Timofeyev, Y. M. Popkov, and N. F. Bakeyev. "Low Angle X-ray Study of the Phase State of Water in Perfluorinated Ion-Exchange Membranes." *Polymer Science U.S.S.R.*, vol. 29, no. 7, pp. 1597–1601, 1987.

7. Ozerin, A. N., A. V. Rebrov, A. N. Yakunin, N. P. Bessonova, N. A. Dreiman, L. F. Sokolov, and N. F. Bakeyev. "Effect of Low Molecular Weight Fractions on the Structure of the Perfluorinated Sulphocationite Ion-Exchange Membrane." *Polymer Science U.S.S.R.*, vol. 28, no. 11, pp. 2559–2565, 1986.

8. Rebrov, A. V., A. N. Ozerin, D. I. Svergun, L. P. Bobrova, and N. F. Bakeyev. "Small Angle X-ray Scatter Study of the Aggregation of Macromolecules of the Perfluorosulphonated Ionomer in Solution." *Polymer Science U.S.S.R.*, vol. 32, no. 8, pp. 1515–1521, 1990.

9. Kumar, S., and M. Pineri. "Interpretation of Small-Angle X-ray and Neutron Scattering Data for Perfluorosulfonated Ionomer Membranes." *Journal of Polymer Science Polymer Physics Edition*, vol. 24, pp. 1767–1782, 1986.

10. Cable, K. M., K. A. Mauritz, and R. B. Moore. *American Chemical Society Polymer Preprints*. Vol. 35, pp. 421–422, 1994.

11. Gebel, G., and J. Lambard. "Small-Angle Scattering Study of Water-Swollen Perfluorinated Ionomer Membranes." *Macromolecules*, vol. 30, pp. 7914–7920, 1997.

12. Gebel, G. "Structural Evolution of Water Swollen Perfluorosulfonated Ionomers From Dry Membrane to Solution." *Polymer*, vol. 41, pp. 5829–5838, 2000.

13. Elliott, J. A., S. Hanna, A. M. S. Elliott, and G. E. Cooley. "Interpretation of the Small-Angle X-ray Scattering From Swollen and Oriented Perfluorinated Ionomer Membranes." *Macromolecules*, vol. 33, pp. 4161–4171, 2000.

14. Elliott, J. A., S. Hanna, A. M. S. Elliott, and G. E. Cooley. "The Swelling Behaviour of Perfluorinated Ionomer Membranes in Ethanol/Water Mixtures." *Polymer*, vol. 42, pp. 2251–2253, 2001.

15. Londono, J. D., R. V. Davidson, and S. Mazur. "SAXS Study of Elongated Ionic Clusters in Poly-Perfluorosulfonic Acid Membranes." *American Chemical Society Polymeric Materials: Science & Engineering Preprints*, vol. 85, no. 2, 2001.

16. Davis, S. V., K. A. Mauritz, and R. B. Moore. "Monitoring of pH as a Control in the Initialization of Perfluorosulfonate Ionomer Membranes." *American Chemical Society Polymer Preprints*, vol. 35, pp. 419, 1994.

17. Glinka, C. J., J. G. Barker, B. Hammouda, S. Krueger, J. J. Moyer, and W. J. Orts. "The 30-m Small-Angle Neutron Scattering Instruments at the National Institute of Standards and Technology." *Journal of Applied Crystallography*, vol. 31, pp. 430–445, 1998.

18. Mackey, E. A., D. L. Anderson, H. Chen-Mayer, R. G. Downing, R. R. Greenberg, G. P. Lamaze, R. M. Lindstrom, D. F. R. Mildner, and R. L. Paul. "Use of Neutron Beams for Chemical Analysis at NIST." *Journal of Radioanalytical and Nuclear Chemistry*, vol. 203, pp. 413–427, 1996.

19. Young, S. K., S. F. Trevino, N. C. Beck Tan, and R. L. Paul. "Utilization of Prompt Gamma Neutron Activation Analysis in the Evaluation of Various Counterion Nafion Membranes." *Journal of Polymer Science Polymer Physics Edition*, March 2001.

20. Young, S. K., S. F. Trevino, N. C. Beck Tan, and R. L. Paul. "Small Angle Neutron Scattering Investigation of Structural Changes in Nafion Membranes Induced by Swelling With Various Solvents." *Journal of Polymer Science Polymer Physics Edition*, April 2001.

21. Klug, H. P., and L. E. Alexander. *X-ray Diffraction Procedures.* New York: John Wiley & Sons, pp. 655–656, 1974.

22. Starkweather, H. W. "Crystallinity in Perfluorosulfonated Acid Ionomers and Related Polymers." *Macromolecules*, vol. 15, pp. 320–323, 1982.

23. Summerfield, G. C., and D. F. R. Mildner. *Journal of Applied Crystallography.* Vol. 16, pp. 384–389, 1983.

24. Litt, M. H. "A Reevaluation of Nafion Morphology." *American Chemical Society Polymer Preprints,* vol. 38, pp. 80–81, 1997.

INTENTIONALLY LEFT BLANK.

REPORT DOCUMENTATION PAGE

Form Approved
OMB No. 0704-0188

1. AGENCY USE ONLY *(Leave blank)*	2. REPORT DATE	3. REPORT TYPE AND DATES COVERED
	November 2002	Interim, June 1999–May 2001

4. TITLE AND SUBTITLE
Morphology and Morphological Changes Within Nafion Membranes Induced by Mechanical Orientation

5. FUNDING NUMBERS
EMAT01/PER

6. AUTHOR(S)
S. F. Trevino and Sandra K. Young

7. PERFORMING ORGANIZATION NAME(S) AND ADDRESS(ES)
U.S. Army Research Laboratory
ATTN: AMSRL-WM-MA
Aberdeen Proving Ground, MD 21005-5069

8. PERFORMING ORGANIZATION REPORT NUMBER
ARL-TR-2700

9. SPONSORING/MONITORING AGENCY NAMES(S) AND ADDRESS(ES)

10.SPONSORING/MONITORING AGENCY REPORT NUMBER

11. SUPPLEMENTARY NOTES

12a. DISTRIBUTION/AVAILABILITY STATEMENT
Approved for public release; distribution is unlimited.

12b. DISTRIBUTION CODE

13. ABSTRACT *(Maximum 200 words)*

The structure of Nafion, a perfluorosulfonated ionomer, has been the subject of many studies. Morphology evaluations have used the methods of small-angle x-ray scattering (SAXS), wide-angle x-ray scattering (WAXS), and small-angle neutron scattering (SANS). Three principal features in the small-angle scattering pattern have been observed on the H+-form Nafion. A peak at approximately Q ~0.2 Å–1 is attributed to the clustering of the acid groups (ionomer peak), that at Q ~0.03 Å–1 to crystalline regions, and an upturn in intensity at the smallest Q to large-scale heterogeneities. Some of the previous works have included samples that have experienced moderate strains by mechanical elongation. In those works, the effect on the ionomer peak has been studied. The WAXS studies led to a model of the packing of the polymer molecules into ionic aggregates, while the SAXS and SANS studies resulted in models of the packing of the ionic clusters. In the present work, SANS measurements on elongated samples of Nafion have been used to obtain data that suggests a model of the structure of the material. The samples studied were elongated at two temperatures, 25° and 155 °C. Although many of the scattering features of these two samples are similar, the samples stretched at 155 °C contain new information concerning the nature of the crystalline region.

14. SUBJECT TERMS	15. NUMBER OF PAGES
Nafion, perfluorosulfonate ionomer membranes, SANS, morphology, pole figures, mechanical orientation	28
	16. PRICE CODE

17. SECURITY CLASSIFICATION OF REPORT	18. SECURITY CLASSIFICATION OF THIS PAGE	19. SECURITY CLASSIFICATION OF ABSTRACT	20. LIMITATION OF ABSTRACT
UNCLASSIFIED	UNCLASSIFIED	UNCLASSIFIED	UL

INTENTIONALLY LEFT BLANK.